We are IntechOpen, the world's leading publisher of Open Access books Built by scientists, for scientists

4,800
Open access books available

122,000
International authors and editors

135M
Downloads

Our authors are among the

154
Countries delivered to

TOP 1%
most cited scientists

12.2%
Contributors from top 500 universities

WEB OF SCIENCE™

Selection of our books indexed in the Book Citation Index in Web of Science™ Core Collection (BKCI)

Interested in publishing with us?
Contact book.department@intechopen.com

Numbers displayed above are based on latest data collected.
For more information visit www.intechopen.com

Chapter 4

Triple Bonds between Bismuth and Group 13 Elements: Theoretical Designs and Characterization

Jia-Syun Lu, Ming-Chung Yang, Shih-Hao Su, Xiang-Ting Wen, Jia-Zhen Xie and Ming-Der Su

Additional information is available at the end of the chapter

http://dx.doi.org/10.5772/67220

Abstract

The effect of substitution on the potential energy surfaces of $RE_{13}{\equiv}BiR$ (E_{13} = B, Al, Ga, In, and Tl; R = F, OH, H, CH_3, SiH_3, Tbt, Ar*, $SiMe(SitBu_3)_2$, and $SiiPrDis_2$) is investigated using density functional theories (M06-2X/Def2-TZVP, B3PW91/Def2-TZVP, and B3LYP/LANL2DZ+dp). The theoretical results suggest that all of the triply bonded $RE_{13}{\equiv}BiR$ molecules prefer to adopt a bent geometry (i.e., $\angle RE_{13}Bi \approx 180°$ and $\angle E_{13}BiR \approx 90°$), which agrees well with the bonding model (model (B)). It is also demonstrated that the smaller groups, such as R = F, OH, H, CH_3, and SiH_3, neither kinetically nor thermodynamically stabilize the triply bonded $RE_{13}{\equiv}BiR$ compounds, except for the case of $H_3SiB{\equiv}BiSiH_3$. Nevertheless, the triply bonded $R'E_{13}{\equiv}BiR'$ molecules that feature bulkier substituents (R' = Tbt, Ar*, $SiMe(SitBu_3)_2$, and $SiiPrDis_2$) are found to have the global minimum on the singlet potential energy surface and are both kinetically and thermodynamically stable. In other words, both the electronic and the steric effects of bulkier substituent groups play an important role in making triply bonded $RE_{13}{\equiv}BiR$ (Group 13–Group 15) species synthetically accessible and isolable in a stable form.

Keywords: bismuth, group 13 elements, triple bond, multiple bond, density functional theory

1. Introduction

Triply bonded molecules are of great interest in structural and synthetic inorganic chemistry as well as in fundamental science. Molecules that have triple bonds, however, pose a more difficult challenge than analogous doubly bonded molecules from a synthetic viewpoint [1–8]. Acetylene is one of the most commonly triply bonded molecules in traditional organic chemistry. Thanks to Kira, Power, Sekiguchi, Tokitoh, Wiberg and many coworkers, the stable

homonuclear alkyne analogues of all of the heavier group 14 elements have now been isolated and characterized [9–19]. Recently, heteronuclear ethyne-like molecules that possess C≡Ge [20, 21], C≡Sn [22], and C≡Pb [23] triple bonds have also been theoretically predicted and have been published elsewhere.

Nevertheless, to the authors' best knowledge, neither experimental nor theoretical studies have been performed on acetylene-like compounds that feature an E_{13}≡Bi (E = B, Al, Ga, In, and Tl) triple bond. It is surprising how little is known about the stability and molecular properties of E_{13}≡Bi, considering the importance of bismuth compounds [24] that contain group 13 elements in inorganic chemistry [25–35] and material chemistry [36–45].

The aim of this study is to theoretically determine the existence and relative stability of RE_{13}≡BiR triply bonded molecules, which can be synthesized as stable compounds when they are properly substituted. For the first time, the structures of RE_{13}≡BiR with various substituents are reported. That is, theoretical calculations of RE_{13}≡BiR are performed, using both smaller ligands (such as, R = F, OH, H, CH_3, and SiH_3) and larger ligands with bulky aryl and silyl groups (i.e., R' = Tbt, Ar*, SiMe(Si*t*Bu$_3$)$_2$, and Si*i*PrDis$_2$; Dis = CH(SiMe$_3$)$_2$; **Scheme 1**) [46–51]. As a result, the effect of substituents on these bismuth-group-13-element triple bonds is systematically investigated using density functional theory (DFT) calculations. It is expected that the theoretical interpretations of the effect of substituents, presented in this work, will help in the experimental preparation of the many precursors of RE_{13}≡BiR.

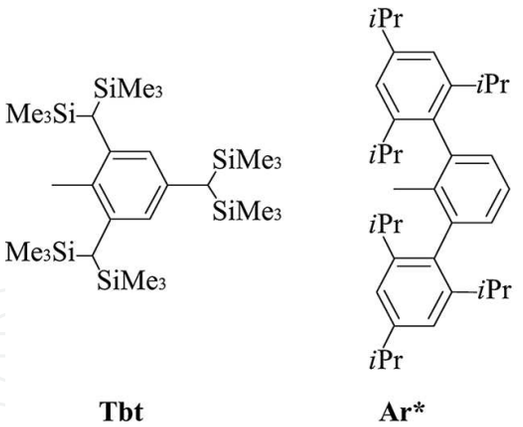

http://dx.doi.org/10.5772/67220

2. Theoretical methods

Geometries were fully optimized using hybrid density functional theory at M06-2X, B3PW91, and B3LYP levels, using the Gaussian 09 program package [52]. It has been reported that M06-2X is proven to have excellent performance for main group chemistry [53]. In both the B3LYP and B3PW91 calculations, Becke's three-parameter nonlocal exchange functional (B3) [54, 55] is used, together with the exact (Hartree-Fock) exchange functional, in conjunction with the nonlocal correlation functional of Lee, Yang, Parr (LYP) [56] and Perdew and Wang (PW91) [57]. Therefore, the geometries of all of the stationary points were fully optimized at the M06-2X, B3PW91, and B3LYP levels of theory. For comparison, the geometries and energetics of the stationary points on the potential energy surface were calculated using the M06-2X, B3PW91, and B3LYP methods, in conjunction with the Def2-TZVP [58] and LANL2DZ+dp [59–62] basis sets. Consequently, these DFT calculations are denoted as M06-2X/Def2-TZVP, B3PW91/Def2-TZVP, and B3LYP/LANL2DZ+dp, respectively.

The spin-unrestricted (UM06-2X, UB3PW91, and UB3LYP) formalisms are used for the open-shell (triplet) species. The $<S^2>$ expectation values for the triplet state for the calculated species all have an ideal value (2.00), after spin annihilation, so their geometries and energetics are reliable for this study. Frequency calculations were performed on all structures, in order to confirm that the reactants and products have no imaginary frequencies, and that the transition states possess only one imaginary frequency. Thermodynamic corrections to 298 K, heat capacity corrections, and entropy corrections (ΔS) are applied at the three DFT levels. Therefore, the relative free energy (ΔG) at 298 K is also calculated at the same levels of theory.

Sequential conformation analyses were performed for each stationary point, for species containing bulky ligands (R' = Tbt, Ar*, SiMe(Si*t*Bu$_3$)$_2$, and Si*i*PrDis$_2$) using Hartree-Fock calculations (RHF/3-21G*). The TbtE$_{13}$≡Bi=Tbt, Ar*=E$_{13}$≡Bi=Ar*, SiMe(Si*t*Bu$_3$)$_2$=E$_{13}$≡Bi=SiMe(Si*t*Bu$_3$)$_2$, and Si*i*PrDis$_2$=E$_{13}$≡Bi=Si*i*PrDis$_2$ (E =B, Al, Ga, In, and Tl) are used as model reactants in this work. It is known that the Hartree-Fock level of theory is insufficient for even a qualitative description of the chemical potential energy surface, so these stationary points were then further calculated at the B3LYP/LANL2DZ+dp level, using the OPT=READFC keyword with a tight convergence option (maximum gradient convergence tolerance = 5.0×10^{-5} hartree/bohr). Because of the limitations of the available CPU time and memory size, frequencies were not calculated for the triply bonded R'E$_{13}$≡BiR' systems with bulky ligands (R') at the B3LYP/LANL2DZ+dp level of theory. As a result, the zero-point energies and the Gibbs free energies for B3LYP/LANL2DZ+dp cannot be applied to these systems.

3. Results and discussion

3.1. Theoretical models for RE$_{13}$≡BiR

In order to understand the bonding interactions in the R=E$_{13}$≡Bi=R molecule, R=E$_{13}$≡Bi=R is divided into one E$_{13}$=R and one Bi=R fragment. The theoretical calculations for these two

fragments indicate that the ground states of E_{13}=R and Bi=R are singlet and triplet states, respectively (vide infra). Therefore, there are two possible interaction modes (A and B) between the E_{13}=R and Bi=R moieties in the formation of the triply bonded R=E_{13}≡Bi=R species, as schematically illustrated in **Figure 1**. In model (A), both E=R and Bi=R units exist as triplet monomers. In this way, the combination between the group 13 element and bismuth can be considered as a triple bond, since it consists of 2 π bonds and 1 donor-acceptor σ bond, for these 2 triplet fragments. As a result, this bonding model allows a linear structure, as shown in **Figure 1(A)**. In model (B), both E_{13}=R and Bi=R units still exist as triplets, so this bonding scheme contains one σ bond and one p-π bond (indicated by two dashed lines), plus one donor-acceptor π-bond because of coupling between the lone pair in Bi=R and the empty p orbital at the E_{13} atom (indicated by the arrow). Accordingly, this bonding pattern results in a bent structure, as shown in **Figure 1(B)**. The importance of the RE_{13}←BiR donor-acceptor interaction is emphasized, as it is essential for the stabilization of the nonlinear structure. These analyses are used to explain the geometrical structures of triply bonded RE_{13}≡BiR species in the following sections.

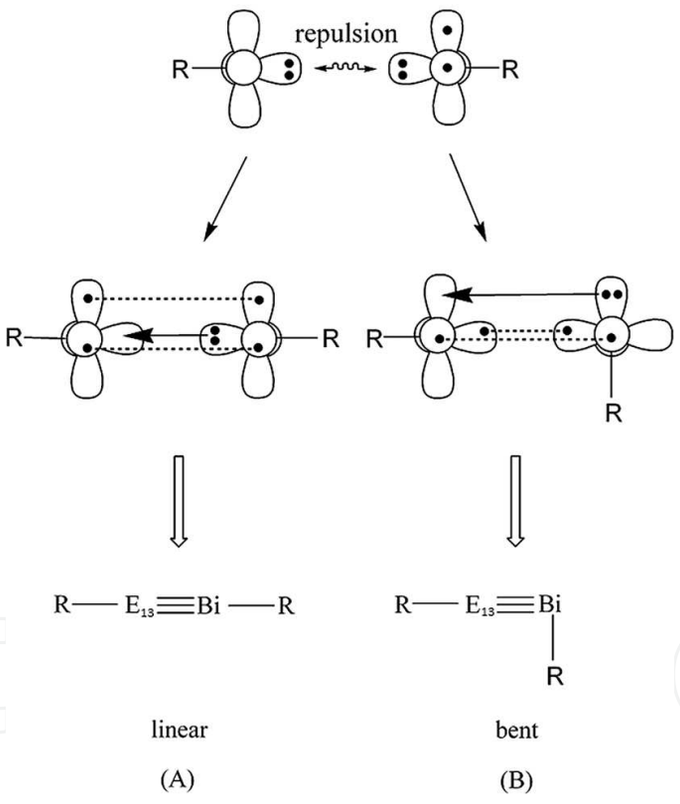

Figure 1. Two interaction models, A and B, in forming triply bonded RE_{13}≡BiR species.

3.2. Small ligands on substituted RE_{13}≡BiR

Small ligands, such as R = F, OH, H, CH_3, and SiH_3, are firstly chosen to study the geometries of the RE_{13}≡BiR (E_{13} = B, Al, Ga, In, and Tl) species. As mentioned in the Introduction, neither experimental nor theoretical results for the triply bonded RE_{13}≡BiR species are available to allow a definitive comparison. As a result, three DFT methods were used (i.e., M06-2X/Def2-

http://dx.doi.org/10.5772/67220

TZVP, B3PW91/Def2-TZVP, and B3LYP/LANL2DZ+dp) to examine their molecular properties. The selected geometrical parameters, natural charge densities (Q_{E13} and Q_{Bi}), binding energies (BE), and Wiberg bond order (BO) [63, 64] are shown in **Table 1** (RB≡BiR), **Table 2** (RAl≡BiR), **Table 3** (RGa≡BiR), **Table 4** (RIn≡BiR), and **Table 5** (RTl≡BiR).

Several important conclusions can be found in **Tables 1–5**, which are shown as follows:

R	F	OH	H	CH_3	SiH_3
B≡Bi (Å)	2.218	2.202	2.091	2.141	2.075
	−2.210	−2.199	−2.083	−2.137	−2.084
	[2.196]	[2.196]	[2.083]	[2.140]	[2.085]
∠R—B—Bi (°)	177.6	176	163.6	176.9	170.9
	−178.8	−175.9	−163.6	−176.9	−169.4
	[178.1]	[176.1]	[163.9]	[174.7]	[171.9]
∠B—Bi—R (°)	80.89	91.96	34.78	90.62	58.89
	−88.58	−90.21	−34.83	−90.26	−58.47
	[87.52]	[89.53]	[38.88]	[99.39]	[59.00]
∠R—B—Bi—R (°)	179.8	77.43	180	173.3	179.7
	−179.1	−75.70	−180.0	−173.5	−179.5
	[179.5]	[76.80]	[180.0]	[179.9]	[180.0]
Q_B (1)	0.1096	−0.0543	−0.3684	−0.3023	−0.5098
	−0.124	(−0.0372)	(−0.2262)	(−0.1390)	(−0.4100)
	[0.2303]	[0.0511]	[−0.1623]	[−0.01010]	[−0.4101]
Q_{Bi} (2)	0.4759	0.3569	0.2189	0.1881	0.1784
	−0.4975	−0.3431	−0.1331	−0.1602	−0.103
	[0.4983]	[0.3552]	[0.1870]	[0.1430]	[0.1520]

Notes: (1) The natural charge density on the central boron atom. (2) The natural charge density on the central bismuth atom. (3) BE = E (triplet state of R=B) + E (triplet state of R=Bi) – E(RB≡BiR). (4) Wiberg bond orders for the B=Bi bonds, see Ref. [18].

Table 1. Selected geometrical parameters, natural charge densities (Q_B and Q_{Bi}), binding energies (BE), and Wiberg bond orders (BO) of RB≡BiR at the M06-2X/Def2-TZVP, B3PW91/Def2-TZVP (in round bracket), and B3LYP/LANL2DZ+dp (in square bracket) levels.

R	F	OH	H	CH_3	SiH_3
Al≡Bi (Å)	2.604	2.606	2.439	2.529	2.501
	(2.601)	(2.601)	(2.463)	(2.539)	(2.532)
	[2.621]	[2.624]	[2.483]	[2.561]	[2.542]
∠R—Al—Bi (°)	176.8	173.4	170.7	177.7	172.5
	(175.4)	(172.9)	(168.1)	(177.6)	(170.4)
	[177.3]	[174.2]	[166.9]	[177.1]	[174.5]

R	F	OH	H	CH_3	SiH_3
∠Al—Bi—R (°)	83.16	84.20	48.09	92.52	62.57
	(84.59)	(85.35)	(49.85)	(92.93)	(61.82)
	[87.00]	[88.32]	[51.00]	[93.77]	[64.03]
∠R—Al—Bi—R (°)	180.0	177.3	180.0	179.9	179.9
	(180.0)	(176.0)	(180.0)	(179.6)	(179.8)
	[180.0]	178.0]	[180.0]	[179.6]	[180.0]
Q_{Al} (1)	0.5031	0.3942	0.1493	0.2692	0.1841
	(0.4904)	(0.3918)	(0.1417)	(0.2544)	(0.2145)
	[0.6664]	[0.4315]	[0.3786]	[0.2414]	[0.1517]
Q_{Bi} (2)	0.3947	0.2709	−0.05788	0.03761	−0.1384
	(0.3196)	(0.1834)	(−0.04954)	(0.02100)	(−0.07446)
	[0.3044]	[0.1982]	[0.03410]	[−0.05262]	[−0.1074]
BE (kcal mol^{-1}) (3)	22.61	20.28	50.55	38.69	53.41
	(30.36)	(31.77)	(85.64)	(63.54)	(57.96)
	[25.47]	[20.51]	[53.65]	[42.77]	[53.47]
Wiberg BO (4)	1.393	1.403	1.746	1.634	1.602
	(1.509)	(1.511)	(1.798)	(1.690)	(1.615)
	[1.521]	[1.516]	[1.787]	[1.706]	[1.653]

Notes: (1) The natural charge density on the central aluminum atom. (2) The natural charge density on the central bismuth atom. (3) BE = E (triplet state of R=Al) + E (triplet state of R=Bi) – E(RAl≡BiR). (4) Wiberg bond orders for the Al=Bi bonds, see Refs. [63, 64].

Table 2. Selected geometrical parameters, natural charge densities (Q_{Al} and Q_{Bi}), binding energies (BE), and Wiberg bond orders (BO) of RAl≡BiR at the M06-2X/Def2-TZVP, B3PW91/Def2-TZVP (in round bracket), and B3LYP/LANL2DZ +dp (in square bracket) levels.

R	F	OH	H	CH_3	SiH_3
Ga≡Bi (Å)	2.639	2.625	2.463	2.543	2.512
	(2.602)	(2.621)	(2.465)	(2.524)	(2.510)
	[2.632]	[2.629]	[2.487]	[2.550]	[2.520]
∠R—Ga—Bi (°)	179.7	175.0	166.5	178.9	178.7
	(178.3)	(173.3)	(166.2)	(177.8)	(177.6)
	[177.3]	[175.5]	[167.0]	[177.3]	[177.0]
∠Ga—Bi—R (°)	86.32	86.85	52.56	91.27	65.56
	(88.49)	(88.52)	(56.24)	(92.86)	(66.28)
	[88.18]	[90.75]	[59.49]	[93.37]	[69.82]
∠R—Ga—Bi—R (°)	179.5	157.1	180.0	179.2	175.8
	(180.0)	(159.8)	(180.0)	(178.8)	(179.9)

http://dx.doi.org/10.5772/67220

R	F	OH	H	CH_3	SiH_3
	[180.0]	[158.0]	[180.0]	[179.3]	[180.0]
Q_{Ga} (1)	0.6246	0.5224	0.2127	0.2266	0.1845
	(0.5012)	(0.3464)	(0.1135)	(0.2356)	(0.1507)
	[0.5700]	[0.3813]	[0.3031]	[0.1984]	[0.07925]
Q_{Bi} (2)	0.3696	0.2435	−0.1367	0.03356	−0.2002
	(0.3574)	(0.2743)	(−0.04212)	(0.05503)	(−0.05512)
	[0.4000]	[0.2395]	[0.06523]	[−0.01620]	[−0.08931]
BE (kcal mol^{-1}) (3)	18.03	16.41	45.28	46.24	46.10
	(22.92)	(26.32)	(79.05)	(60.77)	(49.96)
	[20.80]	[16.61]	[49.49]	[40.12]	[48.61]
Wiberg BO (4)	1.286	1.335	1.718	1.578	1.653
	(1.382)	(1.393)	(1.787)	(1.633)	(1.646)
	[1.403]	[1.431]	[1.758]	[1.656]	[1.673]

Notes: (1) The natural charge density on the central gallium atom. (2) The natural charge density on the central bismuth atom. (3) BE = E (triplet state of R=Ga) + E (triplet state of R=Bi) – E(RGa≡BiR). (4) Wiberg bond orders for the Ga=Bi bonds, see Refs. [63, 64].

Table 3. Selected geometrical parameters, natural charge densities (Q_{Ga} and Q_{Bi}), binding energies (BE), and Wiberg bond orders (BO) of RGa≡BiR at the M06-2X/Def2-TZVP, B3PW91/Def2-TZVP (in round bracket), and B3LYP/LANL2DZ +dp (in square bracket) levels.

R	F	OH	H	CH_3	SiH_3
In≡Bi (Å)	2.804	2.790	2.659	2.696	2.667
	(2.802)	(2.700)	(2.691)	(2.719)	(2.692)
	[2.790]	[2.795]	[2.673]	[2.712]	[2.683]
∠R—In—Bi (°)	179.6	173.9	168.3	179.1	173.8
	(178.0)	(172.2)	(175.2)	(177.3)	(174.3)
	[177.0]	[174.5]	[174.1]	[177.6]	[174.7]
∠In—Bi—R (°)	84.16	85.14	67.00	92.20	70.37
	(87.83)	(89.71)	(77.82)	(94.83)	(75.05)
	[87.43]	[90.79]	[74.35]	[94.16]	[74.37]
∠R—In—Bi—R (°)	179.9	176.1	180.0	178.3	178.9
	(180.0)	(177.3)	(180.0)	(179.1)	(177.5)
	[180.0]	[176.5]	[180.0]	[179.4]	[179.8]
Q_{In} (1)	0.7021	0.6352	0.3755	0.3297	0.3650
	(0.5692)	(0.4640)	(0.2561)	(0.3403)	(0.2872)
	[0.7571]	[0.5053]	[0.4055]	[0.3044]	[0.1756]
Q_{Bi} (2)	0.3973	0.2452	−0.2474	−0.01187	−0.2599

R	F	OH	H	CH_3	SiH_3
	(0.4000)	(0.2511)	(−0.08703)	(0.04410)	(−0.08023)
	[0.3468]	[0.2141]	[0.02620]	[−0.05735]	[−0.1365]
BE (kcal mol^{-1}) (3)	14.66	13.17	39.19	36.87	39.28
	(15.06)	(12.88)	(42.01)	(35.00)	(40.94)
	[18.80]	[13.70]	[44.04]	[35.54]	[41.83]
Wiberg BO (4)	1.312	1.403	1.590	1.543	1.553
	(1.308)	(1.334)	(1.601)	(1.539)	(1.546)
	[1.323]	[1.336]	[1.615]	[1.548]	[1.549]

Notes: (1) The natural charge density on the central indium atom. (2) The natural charge density on the central bismuth atom. (3) BE = E (triplet state of R=In) + E (triplet state of R=Bi) – E(RIn≡BiR). (4) Wiberg bond orders for the In=Bi bonds, see Refs. [63, 64].

Table 4. Selected geometrical parameters, natural charge densities (Q_{In} and Q_{Bi}), binding energies (BE), and Wiberg bond orders (BO) of RIn≡BiR at the M06-2X/Def2-TZVP, B3PW91/Def2-TZVP (in round bracket), and B3LYP/LANL2DZ+dp (in square bracket) levels.

R	F	OH	H	CH_3	SiH_3
Tl≡Bi (Å)	2.859	2.843	2.713	2.742	2.707
	(2.812)	(2.803)	(2.698)	(2.725)	(2.705)
	[2.819]	[2.822]	[2.679]	[2.713]	[2.682]
∠R—Tl—Bi (°)	175.9	173.5	175.7	179.6	174.4
	(178.8)	(172.5)	(176.6)	(178.5)	(174.7)
	[177.2]	[174.4]	[176.3]	[178.5]	[175.9]
∠Tl—Bi—R (°)	81.34	86.72	78.87	91.91	76.03
	(87.73)	(89.82)	(79.00)	(93.54)	(76.50)
	[87.92]	[92.34]	[78.86]	[93.25]	[80.00]
∠R—Tl—Bi—R (°)	180.0	143.7	180.0	172.1	178.9
	(179.9)	(132.9)	(179.9)	(178.6)	(179.9)
	[180.0]	[130.6]	[180.0]	[180.0]	[179.2]
Q_{Tl} (1)	0.6481	0.5672	0.3014	0.4162	0.2665
	(0.6614)	(0.5879)	(0.2284)	(0.2746)	(0.3510)
	[0.7100]	[0.4812]	[0.3536]	[0.2734]	[0.1601]
Q_{Bi} (2)	0.4752	0.3214	−0.1836	0.008121	−0.2245
	(0.3615)	(0.2201)	(−0.05213)	(−0.1282)	(−0.09637)
	[0.3854]	[0.2455]	[0.04813]	[−0.03131]	[−0.1282]
BE (kcal mol^{-1}) (5)	7.90	6.61	30.74	26.94	30.56
	(2.98)	(8.17)	(48.12)	(35.39)	(29.13)

R	F	OH	H	CH_3	SiH_3
	[11.34]	[7.38]	[37.14]	[31.09]	[35.03]
Wiberg BO [6]	1.000	1.132	1.652	1.448	1.792
	(1.121)	(1.254)	(1.765)	(1.514)	(1.824)
	[1.112]	[1.212]	[1.756]	[1.568]	[1.652]

Notes: (1) The natural charge density on the central thallium atom. (2) The natural charge density on the central bismuth atom. (3) BE = E (triplet state of R=Tl) + E (triplet state of R=Bi) – E(RTl≡BiR). (4) Wiberg bond orders for the Tl=Bi bonds, see Refs. [63, 64].

Table 5. Selected geometrical parameters, natural charge densities (Q_{Tl} and Q_{Bi}), binding energies (BE), and Wiberg bond orders (BO) of RTl≡BiR at the M06-2X/Def2-TZVP, B3PW91/Def2-TZVP (in round bracket), and B3LYP/LANL2DZ+dp (in square bracket) levels.

1. As can be seen from **Tables 1–5**, the geometrical parameters of the RE_{13}≡BiR triple bond species are quite analogous at the three levels employed. For instance, the predicted triple bond length for small ligands on RB≡BiR is 2.075–2.218 Å (M06-2X/Def2-TZVP), 2.083–2.210 Å (B3PW91/Def2-TZVP), and 2.083–2.196 Å (B3LYP/LANL2DZ+dp). For RAl≡BiR, the Al≡Bi triple bond length for small ligands is predicted to be 2.439–2.606 Å (M06-2X/Def2-TZVP), 2.463–2.601 Å (B3PW91/Def2-TZVP), and 2.483–2.624 Å (B3LYP/LANL2DZ +dp). For RGa≡BiR, the Ga≡Bi triple bond length for small ligands is predicted to be 2.463–2.639 Å (M06-2X/Def2-TZVP), 2.465–2.621 Å (B3PW91/Def2-TZVP), and 2.487–2.632 Å (B3LYP/LANL2DZ+dp). For RIn≡BiR, the In≡Bi triple bond length for small ligands is predicted to be 2.659–2.804 Å (M06-2X/Def2-TZVP), 2.691–2.802 Å (B3PW91/Def2-TZVP), and 2.673–2.795 Å (B3LYP/LANL2DZ+dp). For RTl≡BiR, the Tl≡Bi triple bond length for small ligands is predicted to be 2.707–2.859 Å (M06-2X/Def2-TZVP), 2.698–2.812 Å (B3PW91/Def2-TZVP), and 2.679–2.822 Å (B3LYP/LANL2DZ+dp).

2. It is apparent from **Tables 1–5** that an acute bond angle ∠E_{13}=Bi=R (close to 90°) in the triply bonded molecule RE_{13}≡BiR is favored. The reason for this can be attributed to the "orbital nonhybridization effect," also known as the "inert *s*-pair effect" [65–68], as discussed previously. Accordingly, these phenomena strongly indicate that mode (B) (**Figure 1**) is preferred in the RE≡BiR molecule, for which bent geometry is favored.

3. The Wiberg bond orders (WBOs) [63, 64] on the substituted RE_{13}≡BiR compounds are also given in **Tables 1–5**. For all the triply bonded RE_{13}≡BiR molecules with small substituents, their WBOs were computed to be less than 2.0, except for the cases of HB≡BiH and (SiH_3)B≡Bi(SiH_3). These WBO values imply that the bonding structure of RE_{13}≡BiR may be due to the resonance structures, [I] and [II]. That is to say, the E_{13}=Bi bond could be either double or triple bonds. From **Tables 1–5**, it seems that the resonance structure [II] prevails for the small ligands on the substituted RE_{13}≡BiR species studied in this work. Indeed, since it is known that the electronegativities decrease in the order B (2.051) > Bi (2.01) > Tl (1.789) > Ga (1.756) > In (1.656) > Al (1.613) [69], the bonding mode of RE_{13}≡BiR should prefer to adopt resonance structure [II] (**Scheme 2**).

With regard to the stability of $RE_{13}BiR$, the results of theoretical calculations on the energy surface of the model $RE_{13}BiR$ (R = F, OH, H, CH_3, and SiH_3) system are depicted in **Figures 2–6**.

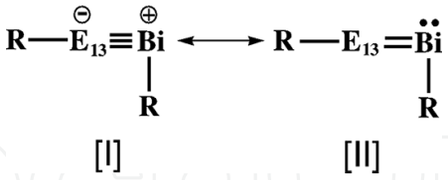

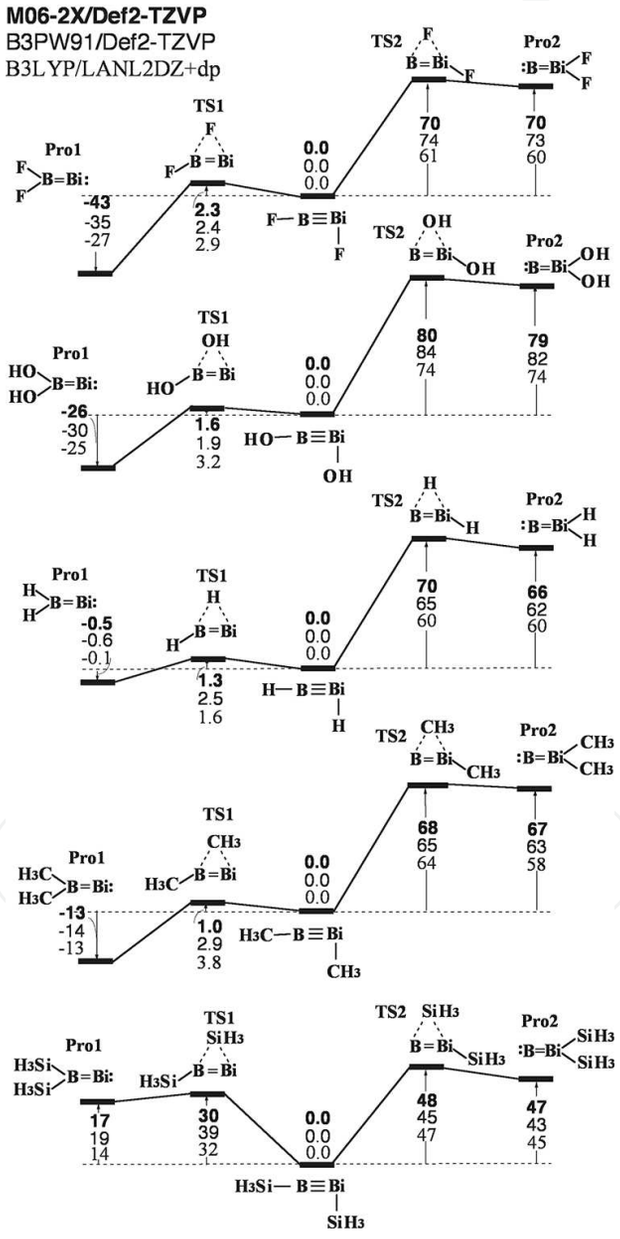

Figure 2. Relative Gibbs free energy surfaces for RB≡BiR (R = F, OH, H, CH_3, and SiH_3). Energies are in kcal/mol, calculated at M06-2X/Def2-TZVP, B3PW91/Def2-TZVP, and B3LYP/LANL2DZ+dp levels of theory. For details see the text and **Table 1**.

http://dx.doi.org/10.5772/67220

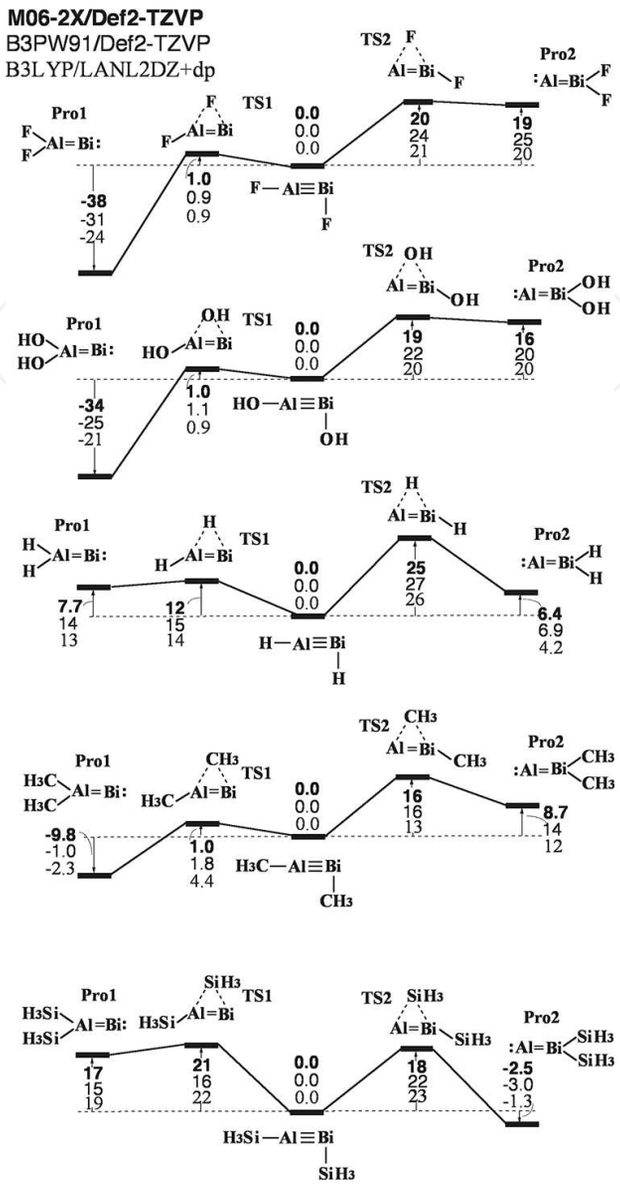

Figure 3. Relative Gibbs free energy surfaces for RAl≡BiR (R = F, OH, H, CH_3, and SiH_3). Energies are in kcal/mol, calculated at M06-2X/Def2-TZVP, B3PW91/Def2-TZVP, and B3LYP/LANL2DZ+dp levels of theory. For details see the text and **Table 2**.

This system exhibits a number of stationary points, including local minima that correspond to RE_{13}≡BiR, R_2E_{13}=Bi:, :E_{13}=BiR_2, and the saddle points connecting them. The transition structures that separate the three stable molecular forms involve a successive unimolecular 1,2-shift TS1 (from RE_{13}≡BiR to R_2E_{13}=Bi:) and a 1,2-shift TS2 (from RE_{13}≡BiR to :E_{13}=BiR_2). As shown in **Figures 1–5**, these theoretical studies using the M06-2X, B3PW91, and B3LYP levels show that the RE_{13}≡BiR species are local minima on the singlet potential energy surface, but they are neither kinetically nor thermodynamically stable for small substituents, except for the case of (SiH_3)B≡Bi(SiH_3). As a result, these triply bonded structures RE_{13}≡BiR seem to be unstable on the singlet energy surface and undergo unimolecular rearrangement to the doubly bonded isomer. In brief, these triply bonded molecules (RE_{13}≡BiR) possessing the small substituents are

predicted to be a kinetically unstable isomer, so these could not be isolated in a matrix or even as transient intermediates.

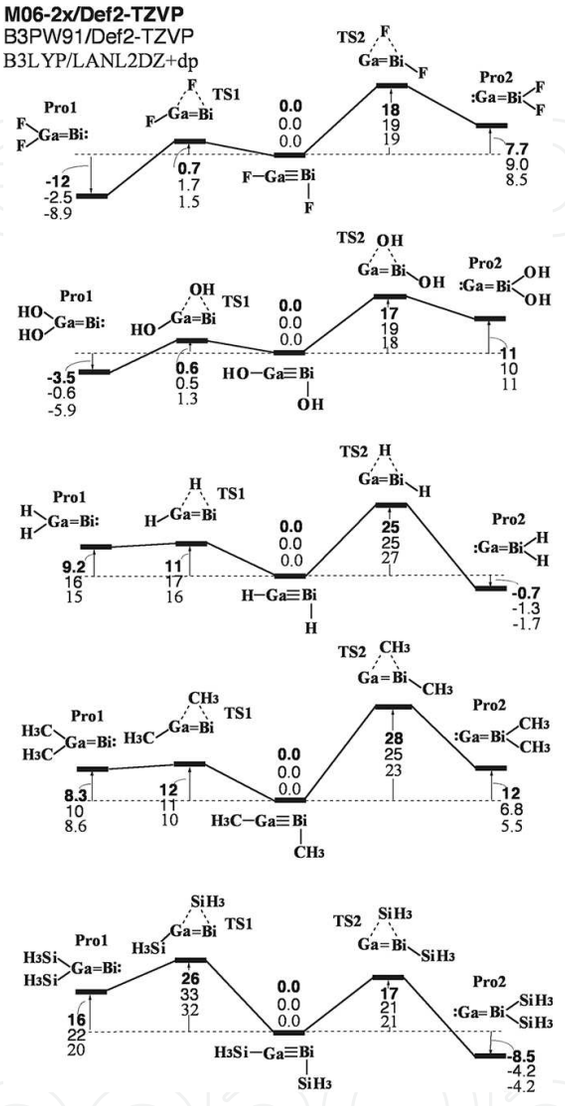

Figure 4. Relative Gibbs free energy surfaces for RGa≡BiR (R = F, OH, H, CH_3, and SiH_3). Energies are in kcal/mol, calculated at M06-2X/Def2-TZVP, B3PW91/Def2-TZVP, and B3LYP/LANL2DZ+dp levels of theory. For details see the text and **Table 3**.

3.3. Large ligands on substituted R'E_{13}≡BiR'

According to the above conclusions for the cases of small substituents, it is necessary to determine whether bulky substituents can destabilize R_2E_{13}=Bi: and :E_{13}=BiR_2 relative to RE_{13}≡BiR (E_{13} = B, Al, Ga, In, and Tl), due to severe steric overcrowding. From **Figure 7**, it is easily anticipated that the presence of extremely bulky substituents at both ends of the RE_{13}≡BiR compounds protects its triple bond from intermolecular reactions, such as polymerization. In order to examine the effect of bulky substituents, the structures of R'E_{13}≡BiR'

optimized for R' = Tbt, Ar*, SiMe(Si*t*Bu$_3$)$_2$, and Si*i*PrDis$_2$ (Scheme 1) at the B3LYP/LANL2DZ +dp level. Selected geometrical parameters, natural charge densities on the central group 13 elements and bismuth (Q_{E13} and Q_{Bi}), binding energies (BE), and Wiberg bond order (BO) [69, 70] are summarized in **Tables 6–10**.

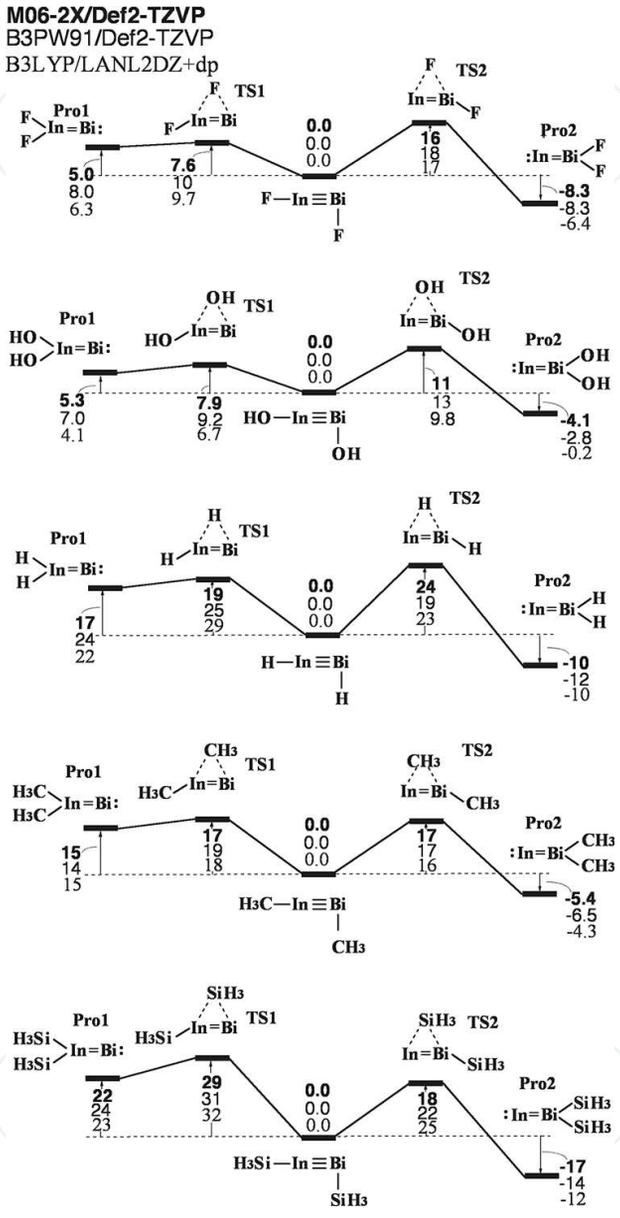

Figure 5. Relative Gibbs free energy surfaces for RIn≡BiR (R = F, OH, H, CH_3, and SiH_3). Energies are in kcal/mol, calculated at M06-2X/Def2-TZVP, B3PW91/Def2-TZVP, and B3LYP/LANL2DZ+dp levels of theory. For details see the text and **Table 4**.

The computational results given in **Tables 6–10** estimate that the E_{13}≡Bi triple bond distances (Å) are about 2.117–2.230 (E_{13} = B), 2.461−2.562 (E_{13} = Al), 2.576–2.580(E_{13} = Ga), 2.615–2.779 (E_{13} = In), and 2.789–2.833 (E_{13} = Tl), respectively. Again, these theoretically predicted values are much shorter than the available experimentally determined E_{13}=Bi single bond lengths

[36, 70–72]. This strongly implies that the central group 13 element (E_{13}) and bismuth in the R'E_{13}≡BiR' (R' = Tbt, Ar*, SiMe(Si*t*Bu$_3$)$_2$, and Si*i*PrDis$_2$) species are triply bonded. Indeed, as shown in **Tables 6–10**, the R'E_{13}≡BiR' molecules accompanied by bulky ligands can effectively produce the triply bonded species. That is, the WBOs in **Tables 6–10** (with larger ligands) are apparently larger than those in **Tables 1–5** (with smaller ligands). Additionally, from **Tables 6–10**, the central E_{13}≡Bi bond lengths calculated for R' = Tbt and Ar* are an average 0.095Å longer than those calculated for R' = SiMe(Si*t*Bu$_3$)$_2$ and Si*i*PrDis$_2$, respectively. The reason for these differences is that the Tbt and Ar* groups are electronegative, but the SiMe(Si*t*Bu$_3$)$_2$ and Si*i*PrDis$_2$ ligands are electropositive. Further, the short length of the E_{13}≡Bi bond in the R'E≡BiR' species can be understood by noting that both SiMe(Si*t*Bu$_3$)$_2$ and Si*i*PrDis$_2$ are more electropositive than the small substituents, as mentioned earlier.

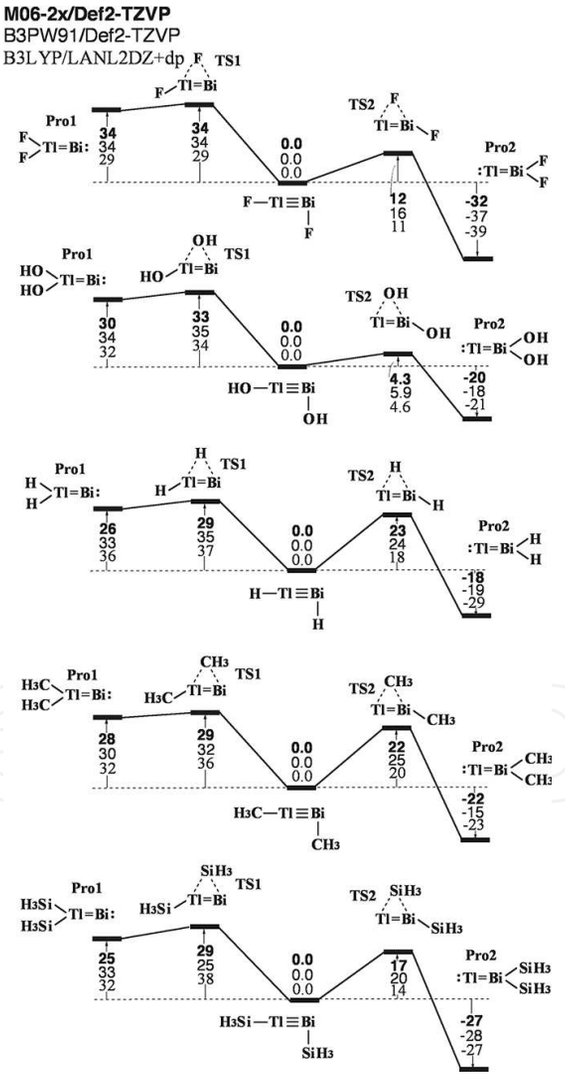

Figure 6. Relative Gibbs free energy surfaces for RTl≡BiR (R = F, OH, H, CH_3, and SiH_3). Energies are in kcal/mol, calculated at M06-2X/Def2-TZVP, B3PW91/Def2-TZVP, and B3LYP/LANL2DZ+dp levels of theory. For details see the text and **Table 5**.

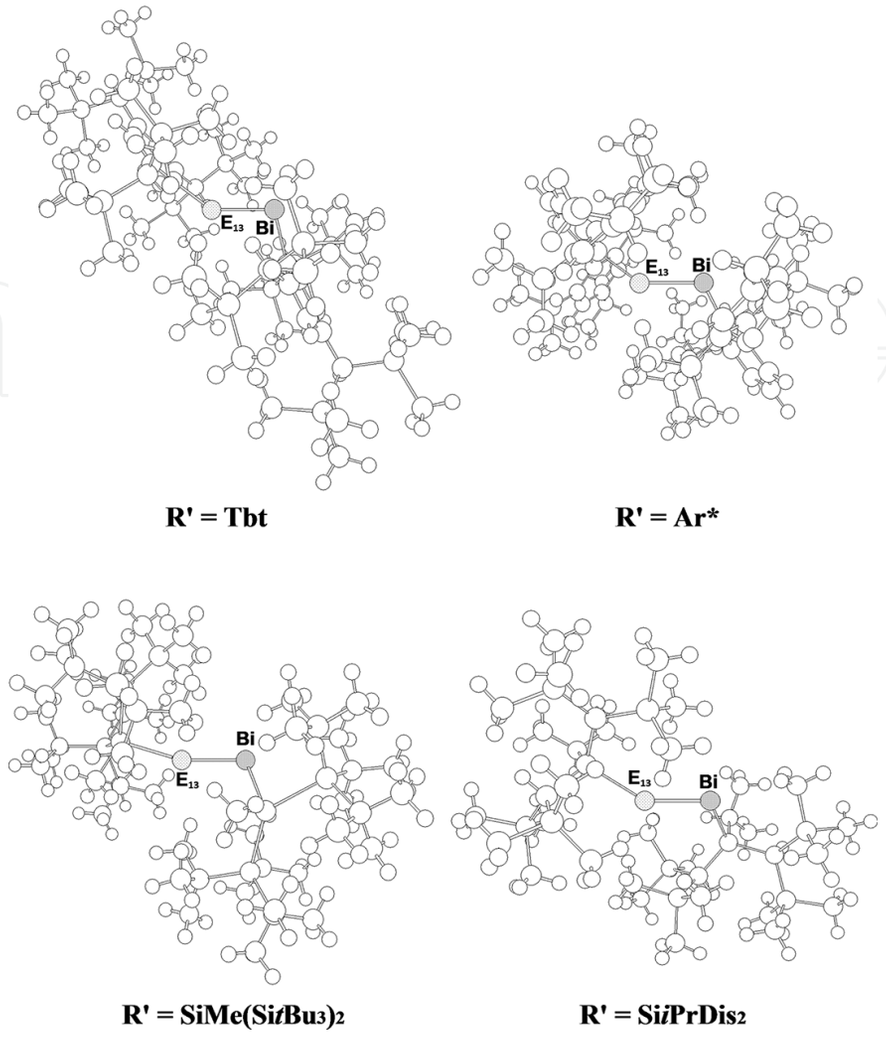

Figure 7. The optimized structures of R'E_{13}≡BiR' (E_{13} = B, Al, Ga, In, and Tl; R' = Tbt, Ar*, SiMe(Si*t*Bu_3)$_2$, and Si*i*PrDis$_2$) at the B3LYP/LANL2DZ+dp level of theory. For details see the text and **Tables 6–10**.

Similar to the small ligands, these DFT results demonstrate that all the R'E_{13}BiR' molecules that possess bulky substituents (R') adopt a bent geometry, as illustrated in **Figure 7**. Our theoretical computations show that model (B), given in **Figure 1**, still predominates and can be used to interpret the geometries of the R'E_{13}≡BiR' systems that bear bulky substituents.

As shown in **Tables 6–10**, the R'E_{13}≡BiR' molecules can be separated into two fragments in solution, when the substituent R' becomes bulkier. The BE that is essential to break the central E_{13}≡Bi bond was computed to be at least > 32 kcal/mol for R' = Tbt, Ar*, SiMe(Si*t*Bu_3)$_2$, and Si*i*PrDis$_2$, for the B3LYP/LANL2DZ+dp method, as given in **Tables 6–10**. These BE values show that the central E_{13} and bismuth elements are strongly bonded and R'E_{13}≡BiR' molecules that contain bulky substituents do not dissociate in solution. Namely, the larger the dissociation energy of the E_{13}≡Bi bond, the shorter and stronger the E_{13}≡Bi triple bond.

As predicted previously, bulky groups destabilize the 1,2-R' migrated isomers because they crowd around one end of the central E_{13}≡Bi bond. As a consequence, the bulky substituents (R') can prevent the isomerization of R'E_{13}≡BiR' compounds, as outlined in **Scheme 3** and

Tables 6–10. The B3LYP/LANL2DZ+dp calculations indicate that the R'E_{13}≡BiR' species with Tbt, Ar*, SiMe(Si*t*Bu$_3$)$_2$, and Si*i*PrDis$_2$ substituents (ΔH_1 and ΔH_2) are at least 56 kcal/mol more stable than the 1,2-R' shifted isomers, respectively. These theoretical results suggest that both doubly bonded R'$_2E_{13}$=Bi: and :E_{13}=BiR'$_2$ isomers are kinetically and thermodynamically unstable, so they rearrange spontaneously to the global minimum R'E_{13}≡BiR' triply bonded molecules, provided that significantly bulky groups are employed.

Theoretical values from the natural bond orbital (NBO) [63, 64] and natural resonance theory (NRT) [73–75] analyses of the R'E_{13}≡BiR' molecules, computed at the B3LYP/LANL2DZ+dp level of theory, are summarized in **Table 11** (E_{13} = B), **Table 12** (E_{13} = Al), **Table 13** (E_{13} = Ga), **Table 14** (E_{13} = In), and **Table 15** (E_{13} = Tl).

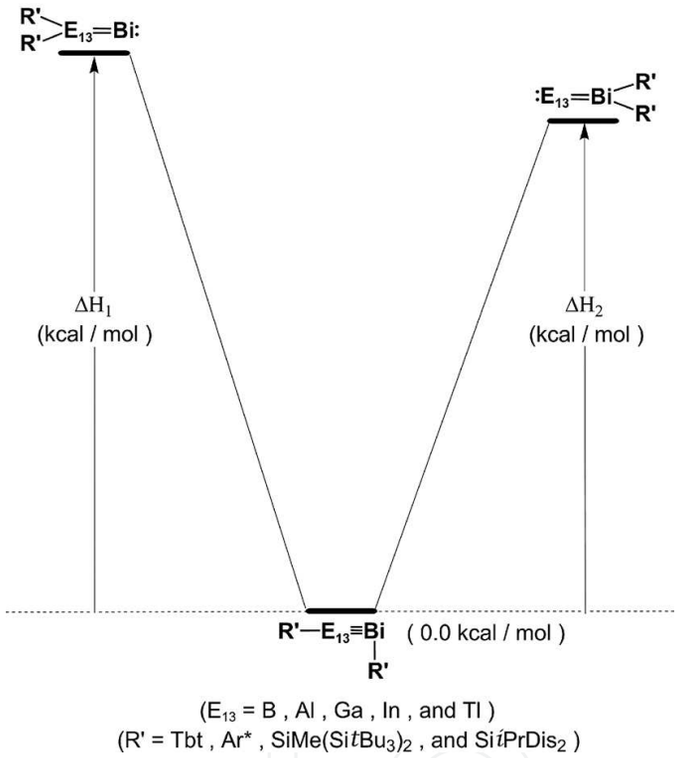

R'	Tbt	Ar*	SiMe(Si*t*Bu$_3$)$_2$	Si*i*PrDis$_2$
B≡Bi (Å)	2.230	2.214	2.117	2.131
∠R'—B—Bi (°)	177.3	110.3	112.9	113.6
∠B—Bi—R' (°)	115.6	115.5	112.5	114.3
∠R'—B—Bi—R' (°)	173.7	172.3	170.4	175.3
Q_B (1)	−0.4310	−0.1711	−0.3251	−0.4742
Q_{Bi} (2)	0.2915	0.3004	0.1426	0.1071
BE (kcal mol^{-1}) (3)	37.58	41.68	36.25	51.07

R'	Tbt	Ar*	SiMe(Si*t*Bu$_3$)$_2$	Si*i*PrDis$_2$
Wiberg BO [4]	2.385	2.249	2.640	2.701
ΔH_1 (kcal mol^{-1}) [5]	62.6	61.04	76.52	77.24
ΔH_2 (kcal mol^{-1}) [6]	98.51	88.38	68.72	78.13

Notes: (1) The natural charge density on the central boron atom. (2) The natural charge density on the central bismuth atom. (3) BE = E (triplet state of B–R') + E (triplet state of Bi–R') – E(R'B≡BiR'). (4) Wiberg Bond Orders for the B–Bi bond, see Refs. [63, 64]. (5) ΔH_1 = E(:B=BiR'$_2$) – E(R'B≡BiR'); see Scheme 3. (6) ΔH_2 = E(R'$_2$B=Bi:) – E(R'B≡BiR'); see **Scheme 3**

Table 6. Geometrical parameters, nature charge densities (Q_B and Q_{Bi}), binding energies (BE), and Wiberg bond order (BO) of R'B≡BiR' at the B3LYP/LANL2DZ+dp level of theory. Also see **Figure 7**.

R'	Tbt	Ar*	SiMe(Si*t*Bu$_3$)$_2$	Si*i*PrDis$_2$
Al≡Bi (Å)	2.562	2.561	2.463	2.461
∠R'—Al—Bi (°)	178.0	113.6	115.4	113.3
∠Al—Bi—R' (°)	113.4	115.5	112.2	109.0
∠R'—Al—Bi—R' (°)	167.1	165.8	173.2	174.7
Q_{Al} [1]	0.4171	0.4111	0.2173	0.1585
Q_{Bi} [2]	0.0773	0.2208	−0.1031	−0.1862
BE (kcal mol^{-1}) [3]	38.62	66.78	33.65	31.76
Wiberg BO [4]	2.092	2.023	2.204	2.259
ΔH_1 (kcal mol^{-1}) [5]	64.52	63.77	77.71	73.68
ΔH_2 (kcal mol^{-1}) [6]	57.43	67.81	71.86	76.62

Notes: (1) The natural charge density on the central aluminum atom. (2) The natural charge density on the central bismuth atom. (3) BE = E (triplet state of Al=R') + E (triplet state of Bi=R') – E(R'Al≡BiR'). (4) Wiberg Bond Orders for the Al=Bi bond, see Refs. [63, 64]. (5) ΔH_1 = E(:Al=BiR'$_2$) – E(R'Al≡BiR'); see Scheme 3. (6) ΔH_2 = E(R'$_2$Al=Bi:) – E(R'Al≡BiR'); see **Scheme 3**.

Table 7. Geometrical parameters, nature charge densities (Q_{Al} and Q_{Bi}), binding energies (BE), and Wiberg bond order (BO) of R'Al≡BiR' at the B3LYP/LANL2DZ+dp level of theory. Also see **Figure 7**.

All the NBO values listed in **Tables 11–15** demonstrate that there exists a weak triple bond, or perhaps a bond between a double and a triple, in the ethyne-like R'E$_{13}$≡BiR' molecule. For instance, the B3LYP/LANL2DZ+dp data for the NBO [63, 64] analyses of the B≡Bi bonding in SiMe(Si*t*Bu$_3$)$_2$=B≡Bi=SiMe(Si*t*Bu$_3$)$_2$, which shows that NBO(B≡Bi) = 0.615(2s2p$^{52.48}$)B + 0.789 (6s6p$^{19.73}$)Bi, strongly suggests that the predominant bonding interaction between the B=SiMe (Si*t*Bu$_3$)$_2$ and the Bi=SiMe(Si*t*Bu$_3$)$_2$ fragments originates from 2p(B) ← 6p(Bi) donation. In other words, boron's electron deficiency and π bond polarity are partially balanced by the donation of the bismuth lone pair into the empty boron p orbital. This, in turn, forms a hybrid π bond. Again, the polarization analyses using the NBO model indicate the presence of the B≡Bi π bonding orbital, 38% of which is composed of natural boron orbitals and 62% of natural bismuth orbitals. There is supporting evidence in **Table 11** that reveals that the B≡Bi triple bond in SiMe(Si*t*Bu$_3$)$_2$=B≡Bi=SiMe(Si*t*Bu$_3$)$_2$ has a shorter single bond character (5.8%) and a

R'	Tbt	Ar*	SiMe(Si*t*Bu$_3$)$_2$	Si*i*PrDis$_2$
Ga≡Bi (Å)	2.578	2.576	2.580	2.579
∠R'—Ga—Bi (°)	178.1	113.4	115.2	112.1
∠Ga—Bi—R' (°)	113.4	115.7	112.0	110.1
∠R'—Ga—Bi—R' (°)	167.9	164.1	175.4	178.5
Q_{Ga} (1)	0.240	0.196	0.069	0.012
Q_{Bi} (2)	0.120	0.261	−0.055	−0.140
BE (kcal mol^{-1}) (3)	43.73	39.28	35.54	32.92
Wiberg BO (4)	2.091	2.181	2.262	2.313
ΔH_1 (kcal mol^{-1}) (5)	68.10	69.08	61.74	58.83
ΔH_2 (kcal mol^{-1}) (6)	78.07	71.28	77.43	64.13

Notes: (1) The natural charge density on the central gallium atom. (2) The natural charge density on the central bismuth atom. (3) BE = E (triplet state of Ga=R') + E (triplet state of Bi=R') – E(R'Ga≡BiR'). (4) Wiberg bond orders for the Ga=Bi bond, see Refs. [63, 64]. (5) ΔH_1 = E(:Ga = BiR'$_2$) – E(R'Ga≡BiR'); see Scheme 3. (6) ΔH_2 = E(R'$_2$Ga=Bi:) – E(R'Ga≡BiR'); see **Scheme 3**.

Table 8. Geometrical parameters, nature charge densities (Q_{Ga} and Q_{Bi}), binding energies (BE), and Wiberg bond order (BO) of R'Ga≡BiR' at the B3LYP/LANL2DZ+dp level of theory. Also see **Figure 7**.

R'	Tbt	Ar*	SiMe(Si*t*Bu$_3$)$_2$	Si*i*PrDis$_2$
In≡Bi (Å)	2.737	2.779	2.615	2.678
∠R'—In—Bi (°)	178.7	111.7	110.0	110.9
∠In—Bi—R' (°)	112.5	113.0	110.6	111.7
∠R'—In—Bi—R' (°)	170.7	174.6	164.3	162.0
Q_{In} (1)	0.299	0.345	0.179	0.101
Q_{Bi} (2)	0.066	0.293	−0.126	−0.132
BE (kcal mol^{-1}) (3)	63.45	45.97	36.20	37.05
Wiberg BO (4)	2.052	2.153	2.211	2.304
ΔH_1 (kcal mol^{-1}) (5)	64.06	60.17	55.72	62.99
ΔH_2 (kcal mol^{-1}) (6)	79.38	61.44	56.03	67.61

Notes: (1) The natural charge density on the central indium atom. (2) The natural charge density on the central bismuth atom. (3) BE = E (triplet state of In=R') + E (triplet state of Bi=R') – E(R'In≡BiR'). (4) Wiberg Bond Orders for the In=Bi bond, see Refs. [63, 64]. (5) ΔH_1 = E(:In = BiR'$_2$) – E(R'In≡BiR'); see Scheme 3. (6) ΔH_2 = E(R'$_2$In=Bi:) – E(R'In≡BiR'); see **Scheme 3.**

Table 9. Geometrical parameters, nature charge densities (Q_{In} and Q_{Bi}), binding energies (BE), and Wiberg bond order (BO) of R'In≡BiR' at the B3LYP/LANL2DZ+dp level of theory. Also see **Figure 7**.

shorter triple bond character (40.1%) but a larger double bond character (54.1%), because the covalent part of the NRT bond order (1.49) is shorter than its ionic part (0.78). The same can also be said of the other three R'B≡BiR' molecules, as shown in **Table 11** as well as other

R'E_{13}≡BiR' compounds represented in **Tables 12–15**. These theoretical evidences strongly suggest that these R'E_{13}≡BiR' species have a weak triple bond.

R'	Tbt	Ar*	SiMe(Si*t*Bu$_3$)$_2$	Si*i*PrDis$_2$
Tl≡Bi (Å)	2.816	2.833	2.820	2.789
∠R'—Tl—Bi (°)	148.2	146.7	164.4	152.4
∠Tl—Bi—R' (°)	116.5	121.4	114.1	125.1
∠R'—Tl—Bi—R (°)	169.5	171.4	176.3	175.8
Q_{Tl} (1)	0.3323	0.4221	0.1504	0.1282
Q_{Bi} (2)	−0.0921	−0.0652	−0.3925	−0.3491
BE (kcal mol^{-1}) (3)	41.66	37.59	36.66	51.07
Wiberg BO (4)	2.081	2.052	2.105	2.128
ΔH_1 (kcal mol^{-1}) (5)	68.66	64.52	63.67	72.12
ΔH_2 (kcal mol^{-1}) (6)	61.54	58.19	68.73	64.61

Notes: (1) The natural charge density on the central thallium atom. (2) The natural charge density on the central bismuth atom. (3) BE = E (triplet state of Tl=R') + E (triplet state of Bi=R') – E(R'Tl≡BiR'). (4) Wiberg bond orders for the Tl=Bi bond, see Refs. [63, 64]. (5) ΔH_1 = E(:Tl = BiR'$_2$) – E(R'Tl≡BiR'); see Scheme 3. (6) ΔH_2 = E(R'$_2$Tl = Bi:) – E(R'Tl≡BiR'); see **Scheme 3**.

Table 10. Geometrical parameters, nature charge densities (Q_{Tl} and Q_{Bi}), binding energies (BE), and Wiberg bond order (BO) of R'Tl≡BiR' at the B3LYP/LANL2DZ+dp level of theory. Also see **Figure 7**.

R′B≡BiR′	WBI	NBO analysis			NRT analysis	
		Occupancy	Hybridization	Polarization	Total/covalent/ionic	Resonance weight
R′=Tbt	2.39	σ = 1.95	σ: 0.7870 B ($sp^{0.90}$) + 0.6170 Bi ($sp^{9.90}$)	61.93% (B)	2.01/1.24/0.77	B=Bi: 12.58%
				38.07% (Bi)		B=Bi: 53.81%
		π = 1.93	π: 0.5938 B ($sp^{1.00}$) + 0.8046 Bi ($sp^{1.00}$)	35.26% (B)		B≡Bi: 33.61%
				64.74% (Bi)		
R′ = Ar*	2.25	σ = 1.94	σ: 0.8058 B ($sp^{0.74}$) + 0.5922 Bi ($sp^{19.46}$)	64.93% (B)	1.95/1.30/0.65	B=Bi: 6.78%
				35.07% (Bi)		B=Bi: 62.97%
		π = 1.90	π: 0.5587 B ($sp^{99.99}$) + 0.8294 Bi ($sp^{64.69}$)	31.22% (B)		B≡Bi: 30.25%
				68.78% (Bi)		
R′ = SiMe (Si*t*Bu$_3$)$_2$	2.64	σ = 1.96	σ: 0.7812 B ($sp^{0.96}$) + 0.6242 Bi ($sp^{10.68}$)	61.03% (B)	2.27/1.49/0.78	B=Bi: 5.77%
				38.97% (Bi)		B=Bi: 54.1%

R′B≡BiR′	WBI	NBO analysis			NRT analysis	
		Occupancy	Hybridization	Polarization	Total/covalent/ ionic	Resonance weight
		π = 1.89	π: 0.6146 B ($sp^{62.48}$) + 0.7889 Bi ($sp^{19.73}$)	37.77% (B) 62.23% (Bi)		B≡Bi: 40.11%
R′ = Si*i*PrDis$_2$	2.7	σ = 1.83	σ: 0.6502 B ($sp^{4.29}$) + 0.7598 Bi ($sp^{1.07}$)	42.27% (B) 57.73% (Bi)	2.31/1.52/0.79	B=Bi: 6.01% B=Bi: 54.39%
		π = 1.80	π: 0.5606 B ($sp^{1.73}$) + 0.8281 Bi ($sp^{4.99}$)	31.43% (B) 68.57% (Bi)		B≡Bi: 39.96%

(1) The Wiberg bond index (WBI) for the B=Bi bond and occupancy of the corresponding σ and π bonding NBO: see Refs. [63, 64], and (2) the natural resonance theory (NRT): see Refs. [73–75].

Table 11. Selected results for the natural bond orbital (NBO) and natural resonance theory (NRT) analyses of R'B≡BiR' compounds that have small substituents, at the B3LYP/LANL2DZ+dp level of theory [1–8, 76–80].

R′Al≡BiR′	WBI	NBO analysis			NRT analysis	
		Occupancy	Hybridization	Polarization	Total/covalent/ ionic	Resonance weight
R′ = Tbt	2.09	σ = 1.98	σ: 0.7538 Al ($sp^{0.15}$) + 0.6571 Bi ($sp^{22.99}$)	56.83% (Al) 43.17% (Bi)	2.12/1.10/1.02	Al=Bi: 12.76% Al=Bi: 75.36%
		π = 1.93	π: 0.4709 Al ($sp^{1.00}$) + 0.8822 Bi ($sp^{1.00}$)	22.17% (Al) 77.83% (Bi)		Al≡Bi: 11.88%
R′ = Ar*	2.02	σ = 1.84	σ: 0.7806 Al ($sp^{0.15}$) + 0.6250 Bi ($sp^{28.77}$)	60.93% (Al) 39.07% (Bi)	2.07/1.01/1.06	Al=Bi: 19.33% Al=Bi: 74.20%
		π = 1.94	π: 0.4960 Al ($sp^{46.09}$) + 0.8673 Bi ($sp^{15.43}$)	24.60% (Al) 75.40% (Bi)		Al≡Bi: 6.47%
R′ = SiMe(Si*t*Bu$_3$)$_2$	2.2	σ = 1.96	σ: 0.7169 Al ($sp^{0.96}$) + 0.6971 Bi ($sp^{21.26}$)	24.70% (Al) 75.30% (Bi)	2.24/1.38/0.86	Al=Bi: 11.69% Al=Bi: 84.51%
		π = 1.89	π: 0.8678 Al ($sp^{19.21}$) + 0.4970 Bi ($sp^{16.37}$)	37.77% (Al) 62.23% (Bi)		Al≡Bi: 3.80%
R′ = Si*i*PrDis$_2$	2.26	σ = 1.86	σ: 0.7184 Al ($sp^{0.93}$) + 0.6956 Bi ($sp^{29.72}$)	51.61% (Al) 48.39% (Bi)	1.91/1.35/0.60	Al=Bi: 12.68% Al=Bi: 83.75%

R′Al≡BiR′	WBI	NBO analysis		NRT analysis		
		Occupancy	Hybridization	Polarization	Total/covalent/ ionic	Resonance weight
		π = 1.90	π: 0.4430 Al ($sp^{59.07}$) + 0.8965 Bi ($sp^{35.38}$)	19.63% (Al) 80.37% (Bi)		Al≡Bi: 3.57%

(1) The Wiberg bond index (WBI) for the Al≡Bi bond and occupancy of the corresponding σ and π bonding NBO: see Refs. [63, 64], and (2) the natural resonance theory (NRT): see Refs. [73–75].

Table 12. Selected results for the natural bond orbital (NBO) and natural resonance theory (NRT) analyses of R'Al≡BiR' compounds that have small substituents, at the B3LYP/LANL2DZ+dp level of theory [1–8, 76–80].

R′Ga≡BiR′	WBI	NBO analysis		NRT analysis		
		Occupancy	Hybridization	Polarization	Total/covalent/ ionic	Resonance weight
R′ = Tbt	2.09	σ = 1.78	σ: 0.7338 Ga ($sp^{1.04}$) + 0.6794 Bi ($sp^{31.81}$)	53.85% (Ga) 46.15% (Bi)	2.09/1.36/0.73	Ga=Bi: 11.42% Ga=Bi: 87.53%
		π = 1.94	π: 0.4586 Ga ($sp^{1.00}$) + 0.8886 Bi ($sp^{1.00}$)	21.04% (Ga) 78.96% (Bi)		Ga≡Bi: 1.05%
R′ = Ar*	2.18	σ = 1.93	σ: 0.8142 Ga ($sp^{0.12}$) + 0.5806 Bi ($sp^{40.52}$)	66.29% (Ga) 33.71% (Bi)	2.05/1.30/0.75	Ga=Bi: 10.87% Ga=Bi: 88.05%
		π = 1.84	π: 0.4810 Ga ($sp^{50.27}$) + 0.8767 Bi ($sp^{14.17}$)	23.13% (Ga) 76.87% (Bi)		Ga≡Bi: 1.08%
R′ = SiMe($Si\mathit{t}Bu_3$)$_2$	2.26	σ = 1.80	σ: 0.7393 Ga ($sp^{0.97}$) + 0.6733 Bi ($sp^{27.39}$)	54.66% (Ga) 67.33% (Bi)	2.11/1.35/0.76	Ga=Bi: 11.84% Ga=Bi: 82.11%
		π = 1.86	π: 0.4937 Ga ($sp^{22.70}$) + 0.8696 Bi ($sp^{17.00}$)	24.38% (Ga) 75.62% (Bi)		Ga≡Bi: 6.05%
R′ = $Si\mathit{i}PrDis_2$	2.31	σ = 1.90	σ: 0.7462 Ga ($sp^{0.92}$) + 0.6657 Bi ($sp^{58.99}$)	55.68% (Ga) 44.32% (Bi)	1.93/1.40/0.53	Ga=Bi: 12.93% Ga=Bi: 80.74%
		π = 1.84	π: 0.4201 Ga ($sp^{99.99}$) + 0.9075 Bi ($sp^{99.99}$)	17.65% (Ga) 82.35% (Bi)		Ga≡Bi: 6.33%

(1) The Wiberg bond index (WBI) for the Ga=Bi bond and occupancy of the corresponding σ and π bonding NBO: see Refs. [63, 64], and (2) the natural resonance theory (NRT): see Refs. [73–75].

Table 13. Selected results for the natural bond orbital (NBO) and natural resonance theory (NRT) analyses of R'Ga≡BiR' compounds that have small substituents, at the B3LYP/LANL2DZ+dp level of theory [1–8, 76–80].

R′In≡BiR′	WBI	NBO analysis			NRT analysis	
		Occupancy	Hybridization	Polarization	Total/covalent/ ionic	Resonance weight
R′ = Tbt	2.05	σ = 1.78	σ: 0.7626 In ($sp^{0.09}$) + 0.6469 Bi ($sp^{50.74}$)	58.15% (In)	2.10/1.15/0.95	In=Bi: 14.33%
				41.85% (Bi)		In=Bi: 76.37%
		π = 1.94	π: 0.4230 In ($sp^{99.99}$) + 0.9061 Bi ($sp^{95.23}$)	17.85% (In)		In≡Bi: 0.93%
				82.11% (Bi)		
R′ = Ar*	2.15	σ = 1.97	σ: 0.7145 In ($sp^{0.07}$) + 0.6996 Bi ($sp^{21.13}$)	51.05% (In)	2.11/1.04/1.07	In=Bi: 11.10%
				48.95% (Bi)		In=Bi: 85.07%
		π = 1.94	π: 0.4774 In ($sp^{99.99}$) + 0.8787Bi ($sp^{99.99}$)	22.79% (In)		In≡Bi: 3.83%
				77.21% (Bi)		
R′ = SiMe($Si\mathit{t}Bu_3$)$_2$	2.21	σ = 1.74	σ: 0.7433 In ($sp^{0.99}$) + 0.6690 Bi ($sp^{35.62}$)	55.25% (In)	2.14/1.22/0.92	In=Bi: 14.20%
				44.75% (Bi)		In=Bi: 81.22%
		π = 1.88	π: 0.4468 In ($sp^{42.13}$) + 0.8696 Bi ($sp^{12.11}$)	19.96% (In)		In≡Bi: 4.58%
				80.04% (Bi)		
R′ = $Si\mathit{i}PrDis_2$	2.3	σ = 1.92	σ: 0.7341 In ($sp^{53.22}$) + 0.6790 Bi ($sp^{0.98}$)	46.11% (In)	1.88/1.27/0.61	In=Bi: 15.31%
				53.89% (Bi)		In=Bi: 81.02%
		π = 1.78	π: 0.4357 In ($sp^{26.46}$) + 0.9001 Bi ($sp^{99.99}$)	18.99% (In)		In≡Bi: 3.67%
				81.01% (Bi)		

Notes: (1) The Wiberg bond index (WBI) for the In=Bi bond and occupancy of the corresponding σ and π bonding NBO: see Refs. [63, 64], and (2) the natural resonance theory (NRT): see Refs. [73–75].

Table 14. Selected results for the natural bond orbital (NBO) and natural resonance theory (NRT) analyses of R'In≡BiR' compounds that have small substituents, at the B3LYP/LANL2DZ+dp level of theory [1–8, 76–80].

R′Tl≡BiR′	WBI	NBO analysis			NRT analysis	
		Occupancy	Hybridization	Polarization	Total/covalent/ ionic	Resonance weight
R′ = Tbt	2.08	σ = 1.96	σ:0.8268 Tl ($sp^{0.07}$) + 0.5625 Bi ($sp^{99.99}$)	68.36% (Tl)	2.15/1.81/0.34	Tl=Bi: 18.71%
				31.64% (Bi)		Tl = Bi: 71.54%
		π = 1.94	π:0.4315 In ($sp^{99.99}$) + 0.9021 Bi ($sp^{99.99}$)	18.61% (In)		Tl≡Bi: 9.75%
				81.37% (Bi)		
R′ = Ar*	2.05	σ = 1.97	σ: 0.8159 Tl ($sp^{0.05}$) + 0.5782 Bi ($sp^{99.99}$)	66.57% (Tl)	2.11/1.70/0.41	Tl=Bi: 21.11%
				33.43% (Bi)		Tl = Bi: 70.15%
		π = 1.95	π: 0.4788 In ($sp^{99.99}$) + 0.8779 Bi ($sp^{99.99}$)	22.92% (In)		Tl≡Bi: 8.74%
				77.08% (Bi)		

R′Tl≡BiR′	WBI	NBO analysis			NRT analysis	
		Occupancy	Hybridization	Polarization	Total/covalent/ ionic	Resonance weight
R′ = SiMe (Si*t*Bu3)2	2.1	σ = 1.98	σ: 0.7986 Tl ($sp^{0.02}$) + 0.6019 Bi ($sp^{31.50}$)	63.77% (Tl) 36.23% (Bi)	2.21/1.40/0.81	Tl=Bi: 16.13% Tl = Bi: 76.20%
		π = 1.92	π: 0.3890 Tl ($sp^{99.99}$) + 0.9212 Bi ($sp^{1.00}$)	15.13% (Tl) 84.87% (Bi)		Tl≡Bi: 7.67%
R′ = Si*i*PrDis2	2.13	σ = 1.98	σ: 0.7757 Tl ($sp^{0.03}$) + 0.6311 Bi ($sp^{23.28}$)	60.17% (Tl) 39.83% (Bi)	1.85/1.23/0.62	Tl=Bi: 20.21% Tl=Bi: 74.69%
		π = 1.91	π: 0.4149 Tl ($sp^{99.99}$) + 0.9099 Bi ($sp^{99.99}$)	17.22% (Tl) 82.78% (Bi)		Tl≡Bi: 5.10%

Notes: (1) The Wiberg bond index (WBI) for the Tl=Bi bond and occupancy of the corresponding σ and π bonding NBO: see Refs. [63, 64], and (2) the natural resonance theory (NRT): see Refs. [73–75].

Table 15. Selected results for the natural bond orbital (NBO) and natural resonance theory (NRT) analyses of R'Tl≡BiR' compounds that have small substituents, at the B3LYP/LANL2DZ+dp level of theory [1–8, 76–80].

4. Overview of RE_{13}≡BiR (E = B, Al, Ga, In, and Tl) systems

This study of the effect of substituents on the possibilities of the existence of triply bonded RE_{13}≡BiR allows the following conclusions to be drawn (**Scheme 4**):

1. The theoretical observations strongly demonstrate that bonding mode (B) is dominant in the triply bonded RE_{13}≡BiR species, since their structures are bent to increase stability, due to electron transfer (denoted by arrows in **Figure 1**) as well as the relativistic effect [65–68].

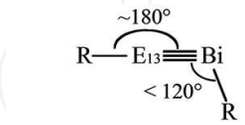

E_{13} = B, Al, Ga, In, and Tl

R = { F, OH, CH_3, H, and SiH_3 ; Tbt, Ar*, SiMe($Si tBu_3$)$_2$, and $Si iPrDis_2$ }

2. The theoretical evidence shows that both the electronic and the steric effects of substituents are crucial to making the E_{13}≡Bi triple bond synthetically accessible. Based on the present theoretical study, however, these E_{13}≡Bi triple bonds should be weak, not as strong as the traditional C≡C triple bond. From our theoretical study, both bulky and electropositive substituents, such as the silyl groups demonstrated in Scheme 1, have a significant effect on the stability of E_{13}≡Bi triply bonded compounds.

Acknowledgements

The authors are grateful to the National Center for High-Performance Computing of Taiwan in providing huge computing resources to facilitate this research. They also thank and the Ministry of Science and Technology of Taiwan for the financial support.

Author details

Jia-Syun Lu[1], Ming-Chung Yang[1], Shih-Hao Su[1], Xiang-Ting Wen[1], Jia-Zhen Xie[1] and Ming-Der Su[1,2]*

*Address all correspondence to: midesu@mail.ncyu.edu.tw

1 Department of Applied Chemistry, National Chiayi University, Chiayi, Taiwan

2 Department of Medicinal and Applied Chemistry, Kaohsiung Medical University, Kaohsiung, Taiwan, Chiayi, Taiwan

References

[1] Power P P. π-Bonding and the lone pair effect in multiple bonds between heavier main group elements. Chem. Rev. 1999; **99**:3463–3504.

[2] Power P P. Silicon, germanium, tin and lead analogues of acetylenes. Chem. Commun. 2003; **17**:2091–2101.

[3] Lein M, Krapp A, Frenking G. Why do the heavy-atom analogues of acetylene E_2H_2 (E = Si-Pb) exhibit unusual structures? J. Am. Chem. Soc. 2005; **127**:6290–6299.

[4] Sekiguchi A, Ichinohe M, Kinjo R. The chemistry of disilyne with a genuine Si–Si triple bond: synthesis, structure, and reactivity. Bull. Chem. Soc. Jpn. 2006; **79**:825–832.

[5] Power P P. Bonding and reactivity of heavier group 14 element alkyne analogues. Organometallics 2007; **26**:4362–4372.

[6] Fischer R C, Power P P. π-bonding and the lone pair effect in multiple bonds involving heavier main group elements: developments in the new millennium. Chem. Rev. 2010; **110**:3877–3923.

[7] Sasamori T, Han J S, Hironaka K, Takagi N, Nagase S, Tokitoh N. Synthesis and structure of stable 1,2-diaryldisilyne. Pure Appl. Chem. 2010; **82**:603–612.

[8] Peng Y, Fischer R C, Merrill W A, Fischer J, Pu L, Ellis B D, Fettinger J C, Herber R H, Power P P. Substituent effects in ditetrel alkyne analogues: multiple vs. single bonded isomers. Chem. Sci. 2010; **1**:461–468.

[9] Sekiguchi A, Kinjo R, Ichinohe M. A stable compound containing a silicon-silicon triple bond. Science 2004; **305**:1755–1757.

[10] Kravchenko V, Kinjo R, Sekiguchi A, Ichinohe M, West R, Balazs Y S, Schmidt A, Karni M, Apeloig Y. Solid-state ^{29}Si nmr study of RSiSiR: a tool for analyzing the nature of the Si-Si bond. J. Am. Chem. Soc. 2006; **128**:14472–14473.

[11] Sasamori T, Hironaka K, Sugiyama T, Takagi N, Nagase S, Hosoi Y, Furukawa Y, Tokitoh N. Synthesis and reactions of a stable 1,2-diaryl-1,2-dibromodisilene: a precursor for substituted disilenes and 1,2-diaryldisilyne. J. Am. Chem. Soc. 2008; **130**:13856–13857.

[12] Wiberg N, Vasisht S K, Fischer G, Mayer P. Disilynes. III [1] a relatively stable disilyne RSi≡SiR (R = $SiMe(SitBu_3)_2$). Z. Anorg. Allg. Chem. 2004; **630**:1823–1828.

[13] Stender M, Phillips A D, Wright R J, Power P P. Synthesis and characterization of a digermanium analogue of an alkyne. Angew. Chem. Int. Ed. 2002; **41**:1785–1787.

[14] Pu L, Phillips A D, Richards A F, Stender M, Simons R S, Olmstead M M, Power P P. Germanium and tin analogues of alkynes and their reduction products. J. Am. Chem. Soc. 2003; **125**:11626–11636.

[15] Stender M, Phillips A. D, Power P P. Formation of $[Ar^*Ge\{CH_2C(Me)C(Me)CH_2\}CH_2C(Me)N]_2$ ($Ar^* = C_6H_3$-2,6-$Trip_2$; Trip = C_6H_2-2,4,6-*i*-Pr_3) via reaction of Ar*GeGeAr* with 2,3-dimethyl-1,3-butadiene: evidence for the existence of a germanium analogue of an alkyne. Chem. Commun. 2002; **12**:1312–1313.

[16] Spikes G H, Power P P. Lewis base induced tuning of the Ge–Ge bond order in a "digermyne". Chem. Commun. 2007; **1**:85–87.

[17] Sugiyama Y, Sasamori T, Hosoi Y, Furukawa Y, Takagi N, Nagase S, Tokitoh N. Synthesis and properties of a new kinetically stabilized digermyne: new insights for a germanium analogue of an alkyne. J. Am. Chem. Soc. 2006; **128**:1023–1031.

[18] Phillips A D, Wright R J, Olmstead M M, Power P P. Synthesis and characterization of 2,6-$Dipp_2$-$H_3C_6SnSnC_6H_3$-2,6-$Dipp_2$ (Dipp = H_3-2,6-Pri_2): a tin analogue of an alkyne. J. Am. Chem. Soc. 2002; **124**:5930–5931.

[19] Pu L, Twamley B, Power P P. Synthesis and characterization of 2,6-$Trip_2H_3C_6PbPbC_6H_3$-2,6-$Trip_2$ (Trip = C_6H_2-2,4,6-*i*-Pr_3): a stable heavier group 14 element analogue of an alkyne. J. Am. Chem. Soc. 2000; **122**:3524–3525.

[20] Liao H-Y, Su M-D, Chu S-Y. A stable species with a formal Ge≡C triple bond — a theoretical study. Chem. Phys. Lett. 2001; **341**:122–128.

[21] Wu P-C, Su M-D. Theoretical designs for germaacetylene (RC≡GeR): a new target for synthesis. Dalton. Trans. 2011; **40**:4253–4259.

[22] Wu P-C, Su M-D. Effects of substituents on the thermodynamic and kinetic stabilities of HCGeX (X = H, CH_3, F, and Cl) isomers. A theoretical study. Inorg. Chem. 2011; **50**:6814–6814.

[23] Wu P-C, Su M-D. A new target for synthesis of triply bonded plumbacetylene (RC≡PbR): a theoretical design. Organometallics 2011; **30**:3293–3301.

[24] Silvestru C, Breunig H J, Althaus H. Structural chemistry of bismuth compounds. I. Organobismuth derivatives. Chem. Rev. 1999; **99**:3277–3328.

[25] Bishop M B, LaiHing K, Cheng P. Y, Pesehke M, Duncan M A. Growth patterns and photoionization dynamics of In/Sb and In/Bi intermetallic clusters. J. Phys. Chem. 1989; **93**:1566–1569.

[26] Itami T, Masaki T, Kuribayasi K, Sato E, Hinada M, Yamasita M, Kawasaki K. Growth of fluctuations under microgravity in liquid Bi-Ga Alloys. J. Non-Cryst. Solids. 1996; **205–207**:375–378.

[27] Mudry S, Korolyshyn A. X-ray study of the structure of liquid Bi-T1. J. Alloys Compd. 1996; **235**:120–123.

[28] Boa D, Ansara I. Thermodynamic assessment of the ternary system Bi-In-Pb. Thermochimica Acta. 1998; **314**:79–86.

[29] Khairulin R A, Stankus S V, Sorokin A L. Determination of the two-melt phase boundary and study of the binary diffusion in liquid Bi–Ga system with a miscibility gap. J. Non-Cryst. Solids. 2002; **297**:120–130.

[30] Xi Y, Zu F-Q, Li X-F, Yu J, Liu L-J, Li Q, Chen Z-H. High-temperature abnormal behavior of resistivities for Bi–In melts. Phys. Lett. 2004; **329**:221–225.

[31] Mangalam R V K, Ranjith R, Iyo A, Sundaresan A, Krupanidhi S B, Rao C N R. Ferroelectricity in $Bi_{26-x}M_xO_{40-\delta}$ (M = Al and Ga) with the γ -Bi_2O_3 structure. Solid State Commun. 2006; **140**:42–44.

[32] Brunetti B, Gozzi D, Iervolino M, Piacente V, Zanicchi G, Parodi N, Borzone G. Bismuth activity in lead-free solder Bi–In–Sn alloys. Comput Coupling Phase Diagr. Thermochem. 2006; **30**:431–442.

[33] Paliwal M, Jung I H. Thermodynamic modeling of the Al–Bi, Al Sb, Mg–Al–Bi and Mg–Al–Sb systems. Comput Coupling Phase Diagr. Thermochem. 2010; **34**:51–63.

[34] Gupta U, Reveles J U, Melko J J, Khanna S N, Castleman Jr. A. W. Origins of stability in mixed bismuth-indium clusters. J. Phys. Chem. C 2010; **114**:15963–15972.

[35] Aksöz S, Ocak Y, Maraşlı N, Keşlioğlu K. Thermal conductivity and interfacial energy of solid Bi solution in the Bi–Al–Zn eutectic system. Fluid Phase Equilib. 2010; **293**:32–41.

[36] Barbier J, Penin N, Cranswick L M. Melilite-type borates $Bi_2ZnB_2O_7$ and $CaBiGaB_2O_7$. Chem. Mater. 2005; **17**:3130–3136.

[37] Curtarolo S, Kolmogorov A N, Cocks F H. High-throughput ab initio analysis of the Bi–In, Bi–Mg, Bi–Sb, In–Mg, In–Sb, and Mg–Sb systems. Comput. Coupling Phase Diagr. Thermochem. 2005; **29**:155–161.

[38] Li Z, Knott S, Mikula A. Calorimetric investigations of liquid Bi–In–Zn alloys. Acta Materialia 2007; **55**:2417–2422.

[39] Madouri D, Ferhat M. How do electronic properties of conventional III–V semiconductors hold for the III–V boron bismuth BBi compound? Phys Stat Sol. 2005; **242**:2856–2863.

[40] Gave M A, Malliakas C D, Weliky D P, Kanatzidis M G. Wide compositional and structural diversity in the system Tl/Bi/P/Q (Q = S, Se) and observation of vicinal P–Tl J coupling in the solid state. Inorg. Chem. 2007; **46**:3632–3644.

[41] Witusiewicz V T, Hecht U, Böttger B, Rex S. Thermodynamic re-optimisation of the Bi–In–Sn system based on new experimental data. J. Alloys Compounds. 2007; **428**:115–124.

[42] Sun Z, Zhu Z, Gao Z, Tang Z. Experimental and theoretical investigation on binary anionic clusters of Al(m)Bi(n)(-). Rapid Commun. Mass Spectrom. 2009; **23**:2663–2668.

[43] Ropero-Vegaa J L, Rosas-Barrerab K L, Pedraza-Avellaa J A, Laverde-Catañob D A, Pedraza-Rosasb J E, Niño-Gómeza M E. Photophysical and photocatalytic properties of Bi_2MNbO_7 (M = Al, In, Ga, Fe) thin films prepared by dip-coating. Mater. Sci. Eng. 2010; **174**:196–199.

[44] Geng L, Cheng W D, Lin C S, Zhang W L, Zhang H, He Z Z. Syntheses, crystal and electronic structures, and characterizations of quaternary antiferromagnetic sulfides: Ba_2MFeS_5 (M = Sb, Bi). Inorg. Chem. 2011; **50**:2378–2384.

[45] Rosas-Barrera K L, Pedraza-Avella J A, Ballén-Gaitán B P, Cortés-Peña J, Pedraza-Rosas J E, Laverde-Cataño D A. Photoelectrolytic hydrogen production using Bi_2MNbO_7 (M = Al, Ga) semiconductor film electrodes prepared by dip-coating. Mater. Sci. Eng. 2011; **176**:1359–1363.

[46] Kobayashi K, Nagase S. Silicon−silicon triple bonds: do substituents make disilynes synthetically accessible? Organometallics 1997; **16**:2489–2491.

[47] Nagase S, Kobayashi K, Takagi N. Triple bonds between heavier group 14 elements. A theoretical approach. J. Organomet. Chem. 2000; **611**:264–271.

[48] Kobayashi K, Takagi N, Nagase S. Do bulky aryl groups make stable silicon−silicon triple bonds synthetically accessible? Organometallics 2001; **20**:234–236.

[49] Takagi N, Nagase S. Substituent Effects on germanium−germanium and tin−tin triple bonds. Organometallics 2001; **20**:5498–5000.

[50] Takagi N, Nagase S. A silicon–silicon triple bond surrounded by bulky terphenyl groups. Chem. Lett. 2001; **30**:966–967.

[51] Takagi N, Nagase S. Theoretical study of an isolable compound with a short silicon-silicon triple bond, $(tBu_3Si)_2MeSiSi{\equiv}SiSiMe(SitBu_3)_2$. Eur. J. Inorg. Chem. 2002;**2002**: 2775–2778.

[52] Frisch M J, Trucks G W, Schlegel H B, Scuseria G E, Robb M A, Cheeseman J R, Scalmani G, Barone V, Mennucci B, Petersson G A, Nakatsuji H, Caricato M, Li X, Hratchian H P,

Izmaylov A F, Bloino J, Zheng G, Sonnenberg J L, Hada M, Ehara M, Toyota K, Fukuda R, Hasegawa J, Ishida M, Nakajima T, Honda Y, Kitao O, Nakai H, Vreven T, Montgomery Jr. J A, Peralta J E, Ogliaro F, Bearpark M, Heyd J J, Brothers E, Kudin K N, Staroverov V N, Keith T, Kobayashi R, Normand J, Raghavachari K, Rendell A, Burant J C, Iyengar S S, Tomasi J, Cossi M, Rega N, Millam J M, Klene M, Knox J E, Cross J B, Bakken V, Adamo C, Jaramillo J, Gomperts R, Stratmann R E, Yazyev O, Austin A J,Cammi R, Pomelli C, Ochterski J W, Martin R L, Morokuma K, Zakrzewski V G, Voth G A, Salvador P, Dannenberg J J, Dapprich S, Daniels A D, Farkas O, Foresman J B, Ortiz J V, Cioslowski J, Fox D J. Gaussian, Inc., Wallingford, CT; 2013.

[53] Zhao Y, Truhlar D G. Density functionals with broad applicability in chemistry. Acc. Chem. Res. 2008; **41**:157–167.

[54] Becke A D. Density-functional exchange-energy approximation with correct asymptotic behavior. Phys. Rev. A 1988; **38**:3098–3100.

[55] Becke A D. Density-functional thermochemistry. III. The role of exact exchange. J. Chem. Phys. 1993; **98**:5648–5652.

[56] Lee C, Yang W, Parr R G. Development of the Colle-Salvetti correlation-energy formula into a functional of the electron density. Phys. Rev. B 1998; **37**:785–789.

[57] Perdew J P, Wang Y. Accurate and simple analytic representation of the electron-gas correlation energy. Phys. Rev. B 1992; **45**:13244–13249.

[58] Weigend F, Ahlrichs R. Balanced basis sets of split valence, triple zeta valence and quadruple zeta valence quality for H to Rn: design and assessment of accuracy. Phys. Chem. Chem. Phys. 2005; **7**:3297–3305.

[59] Hay P J, Wadt W R. Ab initio effective core potentials for molecular calculations. Potentials for the transition metal atoms Sc to Hg. J. Chem. Phys. 1985; **82**:270–283.

[60] Hay P J, Wadt W R. Ab initio effective core potentials for molecular calculations. Potentials for main group elements Na to Bi. J. Chem. Phys. 1985; **82**:284–298.

[61] Hay P J, Wadt W R. Ab initio effective core potentials for molecular calculations. Potentials for K to Au including the outermost core orbitals. J. Chem. Phys. 1985; **82**:299–310.

[62] Check C E, Faust T O, Bailey J M, Wright B J, Gilbert T M, Sunderlin L S. Addition of polarization and diffuse functions to the LANL2DZ basis set for p-block elements. J. Phys. Chem. A 2001; **105**:8111–8116.

[63] Wiberg K B. Application of the pople-santry-segal CNDO method to the cyclopropylcarbinyl and cyclobutyl cation and to bicyclobutane. Tetrahedron 1968; **24**:1083–1096.

[64] Reed A E, Curtiss L A, Weinhold F. Intermolecular interactions from a natural bond orbital, donor-acceptor viewpoint. Chem. Rev. 1988; **88**:899–926.

[65] Pyykkö P, Desclaux J-P. Relativity and the periodic system of elements. Acc. Chem. Res. 1979; **12**:276–281.

[66] Kutzelnigg W. Chemical bonding in higher main group elements. Angew. Chem. Int. Ed. Engl. 1984; **23**:272–295.

[67] Pyykkö P. Relativistic effects in structural chemistry. Chem. Rev. 1988; **88**:563–594.

[68] Pyykkö P. Strong closed-shell interactions in inorganic chemistry. Chem. Rev. 1997; **97**:597–636.

[69] Allen L C. Electronegativity is the average one-electron energy of the valence-shell electrons in ground-state free atoms. J. Am. Chem. Soc. 1989; **111**:9003–9014.

[70] Jones C. Recent developments in low coordination organo-antimony and bismuth chemistry. Coord. Chem. Rev. 2001; **215**:151–169.

[71] Geng L, Cheng W D, Lin C S, Zhang W L, Zhang H, He Z Z. Syntheses, crystal and electronic structures, and characterizations of quaternary antiferromagnetic sulfides: Ba_2MFeS_5 (M = Sb, Bi). Inorg. Chem. 2011; **50**:5679–5686.

[72] Chattopadhyay A, Das K K. Electronic states of TlX (X = As, Sb, Bi): a configuration interaction study. J. Phys. Chem. A 2004; **108**:7306–7317.

[73] Glendening E D, Weinhold F. Natural resonance theory: I. General formalism. J. Comp. Chem. 1998; **19**:593–609.

[74] Glendening E D, Weinhold F. Natural resonance theory: II. Natural bond order and valency. J. Comp. Chem. 1998; **19**:610–627.

[75] Glendening E D, Badenhoop J K, Weinhold F. Natural resonance theory: III. Chemical applications. J. Comp. Chem. 1998; **19**:628–646.

[76] Bino A, Ardon M, Shirman E. Formation of a carbon-carbon triple bond by coupling reactions in aqueous solution. Science 2005; **308**:234–235.

[77] Su P, Wu J, Gu J, Wu W, Shaik S, Hiberty P C. Bonding conundrums in the c2 molecule: a valence bond study. J. Chem. Theory Comput. 2011; **7**:121–130.

[78] Ploshnik E, Danovich D, Hiberty P C, Shaik S. The nature of the idealized triple bonds between principal elements and the σ origins of trans-bent geometries—a valence bond study. J. Chem. Theory Comput. 2011; **7**:955–968.

[79] Danovich D, Bino A, Shaik S. Formation of carbon−carbon triply bonded molecules from two free carbyne radicals via a conical intersection. J. Phys. Chem. Lett. 2013; **4**:58–64.

[80] Kuczkowski A, Thomas F, Schulz S, Nieger M. Synthesis and X-ray crystal structures of novel Al–Bi and Ga–Bi compounds. Organometallics 2000; **19**:5758–5762.

IntechOpen